Pointwise A Posteriori Error Estimators for Multiple and Clustered Eigenvalue Computations

Zhenglei Li¹, Qigang Liang¹, and Xuejun Xu^{1,*}

¹School of Mathematical Science, Tongji University, Shanghai 200092, China and Key Laboratory of Intelligent Computing and Applications (Tongji University), Ministry of Education (2211186@tongji.edu.cn, qigang_liang@tongji.edu.cn, xuxj@tongji.edu.cn)

Abstract: In this work, we propose an a pointwise a posteriori error estimator for conforming finite element approximations of eigenfunctions corresponding to multiple and clustered eigenvalues of elliptic operators. It is proven that the pointwise a posteriori error estimator is reliable and efficient, up to some logarithmic factors of the mesh size. The constants involved in the reliability and efficiency are independent of the gaps among the targeted eigenvalues, the mesh size and the number of mesh level. Specially, we obtain a by-product that edge residuals dominate the a posteriori error in the sense of L^{∞} -norm when the linear element is used. With the aid of the weighted Sobolev stability of the L^2 -projection, we also propose a new method to prove the reliability of the a posteriori error estimator for higher order finite elements. A key ingredient in the a posteriori error analysis is some new estimates for regularized derivative Green's functions. Some numerical experiments verify our theoretical results.

Keywords: Elliptic eigenvalue problems, multiple and clustered eigenvalues, maximum norm, finite element methods, a posteriori error estimator

1 Introduction

This paper considers an a posteriori error estimator for conforming finite element approximations of eigenfunctions corresponding to multiple and clustered eigenvalues of elliptic operators with adaptive finite element methods (AFEMs) in the sense of L^{∞} -norm. When solving elliptic partial differential equations, standard finite element methods on quasi-uniform meshes often exhibit suboptimal performance due to local singularities in the exact solution, which can significantly degrade numerical accuracy. To address this limitation, adaptive finite element methods (AFEMs) were introduced in [3]. Over the past several decades, AFEMs have been the subject of extensive theoretical research and have been successfully implemented in various practical applications, as documented in [2, 4, 8, 9] and the references therein. In the context of elliptic eigenvalue problems, a posteriori error estimators have been rigorously analyzed in [7, 22, 23, 26], where both the reliability and efficiency of these estimators are established. The convergence of AFEMs and the quasi-optimal convergence rate are obtained in [11, 20, 24], the proofs in which are restricted to simple eigenvalues. It is noteworthy that the authors in [10] first derive the a posteriori error estimator for multiple eigenvalues and prove the convergence of AFEMs. Subsequently, the results are extended to clustered eigenvalues in [7, 19].

The a posteriori error estimates discussed above are measured with respect to the energy norm, ensuring convergence of the discrete solution to the exact solution in an integral-averaged sense. However, it should be noted that in many practical applications, pointwise error estimate is of considerable importance (see, for example, [17, 27, 32] and the references therein). Consequently, the development and rigorous analysis of pointwise a posteriori error estimators in the L^{∞} -norm attract significant interest, which often poses substantial theoretical challenges. In recent years, significant progress has been made

in the a priori error analysis in the L^{∞} -norm for finite element approximations of elliptic source problems. A comprehensive overview of these developments can be found in [5, 14, 28, 30, 34, 35] and references therein. Regarding the a posteriori error estimation, the author in [31] introduces pointwise a posteriori error estimators over general polygonal domains in \mathbb{R}^2 and establishes their equivalence to the a priori error, measured by the L^{∞} -norm. Subsequently, these findings have been extended to three-dimensional settings and non-conforming finite element methods in [12]. A crucial step in the proof of the reliability presented in [31] involves deriving an a priori $W^{2,1}$ -estimate for regularized Green's functions. In the context of pointwise a priori error analysis for eigenvalue problems, the study [36] achieves a sharp convergence rate in convex domains, under the assumption that $u \in W^{2,\infty}(\Omega)$. For pointwise a posteriori error of symmetric elliptic eigenvalue problems, we recently (see [29]) design and analyze a pointwise a posteriori error estimator for eigenfunctions corresponding to simple eigenvalues. In practical computations, the pointwise a posteriori error estimator for eigenfunctions corresponding to simple eigenvalues can not capture well the singularities of eigenfunctions corresponding to multiple and clustered eigenvalues (see subsection 5.3). Therefore, it is significant to design and analyze the a posterior error estimator for eigenfunctions corresponding to multiple and clustered eigenvalues.

In this work, we introduce a pointwise a posteriori error estimator and establish its reliability and efficiency with respect to the L^{∞} -norm for eigenfunctions corresponding to multiple and clustered eigenvalues of symmetric elliptic operators. It is noted that analyzing the reliability and efficiency of the pointwise a posteriori error estimator is nontrivial. One first requires to analyze the relationship between constants (involved in the efficiency and reliability) and the gaps among targeted eigenvalues. Hence, it is necessary to estimate the angle between the exact invariant subspace and the discrete invariant subspace in the sense of L^{∞} -norm, which poses more difficulties. The second difficulty arises from the distinction between eigenvalue problems and source problems, the absence of Galerkin orthogonality in the finite element discretization of eigenvalue problems, leads to a L^2 -term, which must be carefully bounded. Third, the extension to higher-order methods needs a more careful estimate for element residuals in the a posteriori error estimator for multiple and clustered eigenvalues.

To overcome these difficulties and obtain the reliability and efficiency of the a posteriori error estimator for eigenfunctions corresponding to multiple and clustered eigenvalues in the sense of L^{∞} -norm, we take advantage of some mathematical tools and skills. A key ingredient is to derive some a priori estimates for the Ritz projection of regularized derivative Green's functions. Moreover, with the help of the weighted Sobolev stability of the L^2 -projection, we provide a new method to extend the a posteriori error analysis to higher-order finite elements, which is different from [6]. Specifically, we obtain the following result:

$$||e_j||_{L^{\infty}(\Omega)} \lesssim \frac{|\ln \underline{h}_l|^2}{|\ln \overline{h}_l|} \frac{\lambda_{n+L}}{\lambda_{n+1}} \eta_l$$

for any $j \in J$ and

$$\eta_l \lesssim \sqrt{L} \sum_{j \in J} ||e_j||_{L^{\infty}(\Omega)},$$

where $e_j = u_j - \Lambda_l u_j$ with u_j being the jth eigenfunction and Λ_l being defined in (2.5), η_l is the pointwise a posterior error estimator defined in (4.1), λ_j is the jth eigenvalue of the eigenvalue problem, $J = \{n+1, n+2, ..., n+L\}$ and \overline{h}_l (\underline{h}_l) is the maximum (minimum) of the mesh-size. Throughout this paper, $a \lesssim (\gtrsim)$ b means $a \leq (\geq)$ Cb, where the letter C is generic positive constant independent of the mesh size and the gaps among eigenvalues in a cluster, possibly different at each occurrence. Specially, as a by-product, we prove that edge residuals dominate the a posterori error in the sense of L^{∞} -norm when the linear element is used.

This paper is organized as follows. In section 2, we introduce the model problem and some mathematical notations. Then we review some useful lemmas in [19] and give a lower bound for the a priori error. In section 3, we derive some new a priori estimates for regularized Green's functions and derivative Green's functions. In section 4, we give the main result of this paper, namely, the reliability and efficiency of the pointwise a posteriori error estimator. Some numerical experiments are given to verify our theoretical findings in section 5 and the conclusion is presented in section 6.

2 Preliminaries

2.1 Triangulations and finite element spaces

Let $\Omega \subset \mathbb{R}^2$ be a polygonal domain without restrictions on the size of the interior angels. Let $r_0 = \frac{\pi}{\theta_0}$, where θ_0 is the largest angle among the interior corners of Ω . Throughout this paper, for any subset $\widetilde{\Omega} \subset \Omega$, we use the standard notations for the Sobolev spaces $W^{m,p}(\widetilde{\Omega})$ $(H^m(\widetilde{\Omega}))$ and $W_0^{m,p}(\widetilde{\Omega})(H_0^m(\widetilde{\Omega}))$ (see [1]). Moreover, we denote by $L^p(\widetilde{\Omega})$ and $L^p(\Gamma)$ the usual Lebesgue spaces equipped with the standard norms $\|\cdot\|_{L^p(\widetilde{\Omega})}$ and $\|\cdot\|_{L^p(\Gamma)}$, where $\Gamma \subset \overline{\Omega}$ is a Lipschitz curve.

We use $\{\mathcal{T}_l\}_{l\in\mathbb{N}}$ to denote a shape-regular family of nested conforming meshes over Ω , i.e., there exists a constant γ such that

$$\frac{h_l|_T}{\rho_T} \le \gamma,$$

where the piecewise constant mesh-size function $h_l := h_{\mathcal{T}_l}$ is defined by $h_l|_T := h_T := \text{meas}(T)^{\frac{1}{2}}$ for any element $T \in \mathcal{T}_l$ and ρ_T is the diameter of the biggest ball contained in T. For simplicity, we assume that each element $T \in \mathcal{T}_l$ is a closed set. We set $\overline{h}_l := \max_{T \in \mathcal{T}_l} h_T$ and $\underline{h}_l := \min_{T \in \mathcal{T}_l} h_T$.

Now we introduce the jump operator. Given an interior edge E shared by two elements T_+ and T_- , i.e., $E = \partial T_+ \cap \partial T_-$, for any piecewise function v, we define

$$[v]_E = (v|_{K_+})|_E - (v|_{K_-})|_E$$

and

$$[\![\nabla v]\!]_E = (\nabla v|_{K_+})|_E - (\nabla v|_{K_-})|_E.$$

By convention, if E is a boundary edge, we set

$$[\![v]\!]_E = v|_E, \quad [\![\nabla v]\!]_E = \nabla v|_E.$$

For simplicity, we denote by

$$[\![\frac{\partial v}{\partial n}]\!]_E = [\![\nabla v]\!]_E \cdot n_E,$$

where n_E is the unit outer normal vector of E. The choice of the particular normal is arbitrary, but is considered to be fixed once and for all. In subsequent sections, we will drop the subscript E without causing confusion.

We denote by $P_k(\mathcal{T}_l)$ the set of piecewise polynomial functions of degree $\leq k$ with respect to \mathcal{T}_l . The conforming finite element space V_l^k is defined as

$$V_l^k = P_k(\mathcal{T}_l) \cap H_0^1(\Omega).$$

2.2 Eigenvalue problem and its discretization

We consider the model problem

$$\begin{cases} -\Delta u = \lambda u & \text{in } \Omega, \\ u = 0 & \text{on } \partial \Omega. \end{cases}$$
 (2.1)

For notational convenience, we denote by

$$(\phi, \psi)_{\widetilde{\Omega}} := \int_{\widetilde{\Omega}} \phi \psi \, dx, \quad \langle \phi, \psi \rangle_{\Gamma} := \int_{\Gamma} \phi \psi \, ds.$$

If $\widetilde{\Omega} = \Omega$, we drop the subscript $\widetilde{\Omega}$ in $(\phi, \psi)_{\widetilde{\Omega}}$. The variational form of (2.1) is to find $(\lambda, u) \in \mathbb{R} \times V (:= H_0^1(\Omega))$ such that

$$a(u,v) = \lambda(u,v) \quad \forall \ v \in V, \tag{2.2}$$

where

$$a(v, w) = \int_{\Omega} \nabla v \cdot \nabla w \ dx \quad \forall \ v, w \in V.$$

We use the kth order Lagrangian finite element to discrete problem (2.1). The finite element discretization is to seek discrete eigenpair $(\lambda_l, u_l) \in \mathbb{R} \times V_l (:=V_l^k)$ satisfies

$$a(u_l, v_l) = \lambda_l(u_l, v_l) \quad \forall \ v_l \in V_l. \tag{2.3}$$

It is known that (2.1) has countably many positive eigenvalues, with the only accumulation point $+\infty$. Suppose that the eigenvalues of (2.1) and the discrete eigenvalues of (2.3) are enumerated as

$$0 < \lambda_1 \le \lambda_2 \le \dots$$
 and $0 < \lambda_{l,1} \le \dots \le \lambda_{l,\dim(V_l)}$.

Let $\{u_1, u_2, u_3, \dots\}$ $(\{u_{l,1}, u_{l,2}, \dots, u_{l,\dim(V_l)}\})$ denote some L^2 -orthonormal bases of corresponding (discrete) eigenfunctions. For a cluster of eigenvalues $\lambda_{n+1}, \dots, \lambda_{n+L}$ of length $L \in \mathbb{N}$, we define the index set

$$J := \{n+1, \dots, n+L\}$$

and the spaces

$$W := \operatorname{span}\{u_j\}_{j \in J} \quad \text{and} \quad W_l := \operatorname{span}\{u_{l,j}\}_{j \in J}.$$

We assume that there holds a continuous gap condition, i.e.,

$$\lambda_n < \lambda_{n+1} \le \lambda_{n+2} \le \dots \le \lambda_{n+L} < \lambda_{n+L+1}$$

(with the convention $\lambda_0 := 0$).

2.3 Some basic estimates for eigenvalue clusters

We first introduce some operators. Define the Ritz projection $R_l: V \to V_l$ such that

$$a(R_l v, w_l) = a(v, w_l) \quad \forall \ w_l \in V_l. \tag{2.4}$$

We use $Q_l: L^2(\Omega) \to V_l$ to denote the L^2 -projection defined by

$$(Q_l v, w_l) = (v, w_l) \quad \forall \ w_l \in V_l$$

and $\Pi_l^k: C^0(\overline{\Omega}) \to V_l^k$ to denote the usual Lagrange interpolation operator. Moreover, we denote by P_l the L^2 -projection to W_l . We also denote by Λ_l the composite of P_l and R_l , namely

$$\Lambda_l = P_l \circ R_l. \tag{2.5}$$

For any index $j \in J$, the function $\Lambda_l u_j \in W_l$ is regarded as the approximation of u_j (in subsection 4.2, we explain that it is a reasonable approximation). Note that $\Lambda_l u_j$ is not necessarily an eigenfunction.

Now we shall review some useful results of eigenvalues clusters in [18] and [19]. Here we omit the details.

Lemma 2.1 Assume that there exists a separation bound

$$M_J = \sup_{l \in \mathbb{N}} \max_{i \in \{1, 2, 3, \dots, dim(V_l) \setminus J\}} \max_{j \in J} \frac{\lambda_j}{|\lambda_{l, i} - \lambda_j|} < \infty.$$

$$(2.6)$$

Any eigenfunction $u_j \in W$ $(j \in J)$ with $||u_j||_{L^2(\Omega)} = 1$ satisfies

$$||u_j - \Lambda_l u_j||_{L^2(\Omega)} \le (1 + M_J)||u_j - R_l u_j||_{L^2(\Omega)}. \tag{2.7}$$

Lemma 2.2 Any eigenpair $(\lambda_j, u_j) \in \mathbb{R}^+ \times W \ (j \in J)$ of (2.1) satisfies

$$a(\Lambda_l u_j, v_l) = \lambda_j(P_l u_j, v_l), \quad \forall v_l \in V_l.$$
(2.8)

Besides the above two lemmas, we shall derive an a priori lower bound for $||u_j - \Lambda_l u_j||_{L^{\infty}(\Omega)} (j \in J)$, which will be used in the subsequent a posteriori error analysis.

Lemma 2.3 (Lower bound) Let $(\lambda_j, u_j) \in \mathbb{R}^+ \times W$ $(j \in J)$ be an eigenpair of (2.1). If the mesh-size \overline{h}_l is small enough, we have the lower bound

$$\inf_{v_l \in V_l(\mathcal{T}_l)} \|u_j - v_l\|_{L^{\infty}(\Omega)} \gtrsim \underline{h}_l^{2[\frac{k+1}{2}]},\tag{2.9}$$

where [c] represents the rounding of the number c.

Proof. Let $z \in T_z$ $(T_z \in \mathcal{T}_l)$ satisfy $|u_j(z)| = ||u_j||_{L^{\infty}(\Omega)}$. It is known that the following estimate holds for 1 (see [13, 21]):

$$|v|_{W^{2,p}(\Omega)} \le C_p ||\Delta v||_{L^p(\Omega)} \quad \forall \ v \in W^{2,p}(\Omega) \cap W_0^{1,p}(\Omega).$$
 (2.10)

On using the Sobolev embedding theorem, in conjunction with (2.10), we obtain

$$||u_j||_{C^{0,\alpha_0}(\overline{\Omega})} \lesssim ||\lambda_j u_j||_{L^p(\Omega)} \lesssim 1$$

for some $\alpha_0 > 0$ and 1 . Thus we may infer that

$$d := \operatorname{dist}(z, \partial\Omega) \gtrsim \left(\frac{\|u_j\|_{L^{\infty}(\Omega)}}{\lambda_j}\right)^{\frac{1}{\alpha_0}} \gtrsim 1.$$

Let $k_0 := \left[\frac{k+1}{2}\right]$. We know that u is smooth enough in the interior of Ω . Using the standard interpolation theory and inverse estimates, for any $v \in P_{2k_0-1}(\mathcal{T}_l)$ we may deduce

$$\begin{split} \lambda_j^{k_0} \|u_j\|_{L^\infty(\Omega)} &= |\Delta^{k_0} u_j(z)| \lesssim |u_j|_{W^{2k_0,\infty}(T_z)} \\ &= |u_j - v|_{W^{2k_0,\infty}(T_z)} \\ &\leq |u_j - \Pi_l^{2k_0} u_j|_{W^{2k_0,\infty}(T_z)} + |\Pi_l^{2k_0} u_j - v|_{W^{2k_0,\infty}(T_z)} \\ &\lesssim h_{T_z} |u_j|_{W^{2k_0+1,\infty}(T_z)} + h_{T_z}^{-2k_0} \|\Pi_l^{2k_0} u_j - v\|_{L^\infty(T_z)} \\ &\leq h_{T_z} |u_j|_{W^{2k_0+1,\infty}(T_z)} + h_{T_z}^{-2k_0} (\|u_j - \Pi_l^{2k_0} u_j\|_{L^\infty(T_z)} + \|u_j - v\|_{L^\infty(T_z)}) \\ &\lesssim h_{T_z} |u_j|_{W^{2k_0+1,\infty}(T_z)} + h_{T_z}^{-2k_0} \|u_j - v\|_{L^\infty(T_z)}. \end{split}$$

It follows that

$$\inf_{v_l \in P_{2k_0-1}(\mathcal{T}_l)} \|u_j - v\|_{L^{\infty}(T_z)} \gtrsim h_{T_z}^{2k_0} - h_{T_z}^{2k_0+1} |u_j|_{W^{2k_0+1,\infty}(T_z)}$$

To drop the second term, we use the well-known interior estimate (see Theorem 5 in subsection 6.3.1 in [16])

$$|u_i|_{H^m(U)} \lesssim 1$$

for any positive integer m and $U \subset\subset \Omega$, where we use $U \subset\subset \Omega$ to denote U is a subset of Ω satisfying $\operatorname{dist}(\partial U, \partial \Omega) \gtrsim 1$. By the Sobolev embedding theorem and noting $d \gtrsim 1$, we have

$$|u_j|_{W^{2k_0+1,\infty}(T_z)} \lesssim 1,$$

which leads to (2.9) with a small enough h_l .

3 Some a priori estimates

In this subsection, we introduce a regularized (derivative) Green's function, and derive some useful a priori estimates, which will play an important role in the next section.

3.1 $W^{2,1}$ -estimate for regularized Green's function

Given a fixed point $x_0 \in \overline{\Omega}$, define a smooth function δ_0 satisfying (see [31]):

supp
$$\delta_0 \subset B(x_0, \rho), \quad \int_{\Omega} \delta_0 \, \mathrm{d}x = 1,$$
 (3.1)

and

$$0 \le \delta_0 \lesssim \rho^{-2}, \quad \|\delta_0\|_{W^{s,\infty}(\Omega)} \lesssim \rho^{-s-2}, \quad s = 1, 2, \dots$$
 (3.2)

where $\rho = h_T^{\beta}$ with $\beta \geq 1$ being an undetermined parameter and T is an element containing x_0 . We define the regularized Green's function g_0 such that

$$\begin{cases}
-\Delta g_0 = \delta_0 & \text{in } \Omega, \\
g_0 = 0 & \text{on } \partial\Omega.
\end{cases}$$
(3.3)

For the following analysis, we review an $W^{2,1}$ -estimate for g_0 for arbitrary polygonal domain (see [29])

$$|g_0|_{W^{2,1}(\Omega)} \lesssim |\ln \rho|. \tag{3.4}$$

3.2 Estimates for regularized derivative Green's function

For any element $T \in \mathcal{T}_l$, let $x_T \in T$. There exists $\delta_1 \in C_0^{\infty}(T)$ (see [25, 33]) satisfying

$$(\delta_1, v)_T = v(x_T) \ \forall \ v \in P_k(T), \ \|\delta_1\|_{W^{s,\infty}(\Omega)} \le h_T^{-s-2}, s = 0, 1, 2, \dots$$
 (3.5)

Define a regularized derivative Green's function g_1 scuh that

$$\begin{cases}
-\Delta g_1 = \nabla \delta_1 \cdot \nu, & \text{in } \Omega, \\
g_1 = 0, & \text{on } \partial \Omega,
\end{cases}$$
(3.6)

where $\nu = (\nu_1, \nu_2)$ is an arbitrary unit vector. We introduce the regularized derivative Green's function, which plays a crucial role in the subsequent a posteriori error analysis. We review a result about the gradient estimate in [37], which is beneficial to estimate the $W^{1,p}$ -norm of $g_1(g_0)$.

Lemma 3.1 Given a Lipschitz domain D, let U solve

$$\begin{cases} -\Delta U = \operatorname{div} F & x \in D, \\ U = 0 & x \in \partial D, \end{cases}$$

where $F \in (L^p(D))^2$. We have the following $W^{1,p}$ -estimate

$$||U||_{W^{1,p}(D)} \lesssim ||F||_{L^p(D)},$$
 (3.7)

where $\frac{4}{3} - \varepsilon with <math>\varepsilon > 0$ depending only on D.

Using Lemma 3.1, we may give $W^{1,p}$ -estimates for g_0 and g_1 .

Lemma 3.2 Let g_0 and g_1 be defined as (3.3) and (3.6). The following estimates hold

$$|g_0|_{W^{1,p}(\Omega)} \lesssim 1 \tag{3.8}$$

for 1 , and

$$|g_1|_{W^{1,p}(\Omega)} \lesssim h_T^{\frac{2}{p}-2},$$
 (3.9)

for $\frac{4}{3} - \varepsilon_1 , where <math>\varepsilon_1 > 0$ depends only on Ω .

Proof. We first prove (3.9). Let $\delta_1 \in C_0^{\infty}(T)$ be defined as in (3.5). For any $x \in T$, we denote by l_x the straight line containing x, which is parallel to the x_1 -axis. Let \hat{x} be the leftmost intersection point of l_x and ∂T . We denote by $l_{\hat{x}x}$ the line segment with \hat{x} and x as the endpoints. Define

$$F_1 := \nu_1 \int_{l_{\hat{x}x}} \frac{\partial \delta_1}{\partial x_1} \mathrm{d}s$$

for $x \in T$. For $x \notin T$, we let $F_1 = 0$. It may be seen that

$$\frac{\partial F_1}{\partial x_1} = \nu_1 \frac{\partial \delta_1}{\partial x_1}.$$

Using (3.5), we have

$$||F_1||_{L^p(\Omega)} \lesssim h_T^{\frac{2}{p}-2}$$

for any $1 \leq p \leq \infty$. Similarly, we may define F_2 , which satisfies

$$\frac{\partial F_2}{\partial x_2} = \nu_2 \frac{\partial \delta_1}{\partial x_2}$$

and

$$||F_2||_{L^p(\Omega)} \lesssim h_T^{\frac{2}{p}-2}$$

for any $1 \leq p \leq \infty$. Let $F = (F_1, F_2)$. It is obvious that

$$\operatorname{div} F = \nabla \delta_1 \cdot \nu.$$

Owing to Lemma 3.1, we obtain

$$|g_1|_{W^{1,p}(\Omega)} \lesssim ||F||_{L^p(\Omega)} \lesssim h_T^{\frac{2}{p}-2}$$
 (3.10)

for $\frac{4}{3} - \varepsilon_1 , where <math>\varepsilon_1 > 0$ depends only on Ω . Using a similar argument, we may prove (3.8).

With the help of Lemma 3.2, we may obtain some estimates for R_lg_1 .

Lemma 3.3 It holds that

$$|R_l g_1|_{H^1(\Omega)} \lesssim h_T^{-1}$$
 (3.11)

and

$$||R_l g_1||_{L^2(\Omega)} \lesssim \overline{h}_l^r h_T^{-1} \tag{3.12}$$

for $r < r_0$.

Proof. In conjunction with (3.5) and (3.6), we have

$$|R_{l}g_{1}|_{H^{1}(\Omega)}^{2} = a(R_{l}g_{1}, R_{l}g_{1}) = (R_{l}g_{1}, \nabla \delta_{1} \cdot \nu)$$

= $(\nabla R_{l}g_{1} \cdot \nu, \delta_{1}) \lesssim h_{T}^{-1}|R_{l}g_{1}|_{H^{1}(\Omega)},$

which yields (3.11). By a standard dual argument, we have

$$||g_1 - R_l g_1||_{L^2(\Omega)} \lesssim \overline{h}_l^r |g_1 - R_l g_1|_{H^1(\Omega)} \lesssim \overline{h}_l^r h_T^{-1}$$
 (3.13)

for $r \in (0, r_0)$. Combining (3.9) and (3.13), by the Sobolev embedding theorem, we obtain

$$||R_l g_1||_{L^2(\Omega)} \lesssim ||g_1||_{L^2(\Omega)} + ||g_1 - R_l g_1||_{L^2(\Omega)}$$
$$\lesssim h_T^{\frac{2}{p}-2} + \overline{h}_l^r h_T^{-1}$$

for any $r < r_0$ and $\frac{4}{3} - \varepsilon_0 . Choosing <math>p \le \frac{2}{r+1}$, we get (3.12).

4 A posteriori error analysis

In this section, we propose two pointwise a posteriori error estimators, including computable and theoretical estimators. Specifically, the computable (local) estimator is defined as

$$\eta_l(T) := h_T^2 \sum_{i \in I} \|\lambda_{l,i} u_{l,i} + \Delta u_{l,i}\|_{L^{\infty}(T)} + h_T \sum_{i \in I} \| \left[\frac{\partial u_{l,i}}{\partial n} \right] \|_{L^{\infty}(\partial T \setminus \partial \Omega)}, \quad \eta_l := \max_{T \in \mathcal{T}_l} \eta_l(T), \tag{4.1}$$

and the theoretical estimator associated with the index j is defined as

$$\eta_{l,j}^* := \inf_{v_l \in V_l} \max_{T \in \mathcal{T}_l} \left(h_T^2 \|\Delta \Lambda_l u_j + v_l\|_{L^{\infty}(T)} + h_T \| \left[\frac{\partial \Lambda_l u_j}{\partial n} \right] \|_{L^{\infty}(\partial T \setminus \partial \Omega)} \right). \tag{4.2}$$

For $j \in J$, denote $e_j := u_j - \Lambda_l u_j$ where Λ_l is defined in (2.5). The adaptive algorithm consists of the following process:

Input. Give an initial triangulation \mathcal{T}_0 and the bulk parameter $0 < \theta \le 1$.

for l = 0, 1, 2, ... do

Solve. Compute discrete solutions $(\lambda_{l,j}, u_{l,j})$ for $j \in J$ of (2.3) with respect to \mathcal{T}_l .

Estimate. Compute local contributions of the error estimator $\eta_l(T)$ for all $T \in \mathcal{T}_l$.

Mark. We mark all elements satisfying

$$\eta_l(T) \geq \theta \eta_l$$
.

Refine. Generate a new triangulation \mathcal{T}_{l+1} by using the BiSecLG(1) refinement strategy in [15]. end do

Output. Sequences of triangulations $\{\mathcal{T}_l\}_l$, discrete solutions $\{(\lambda_{l,j}, u_{l,j}\}_{j\in J}\}_l$ and the a posteriori error estimators $\{\eta_l\}_l$.

Remark 4.1 In the subsequent analysis for the reliability of η_l , we will use the weighted Sobolev stability of Q_l in the sense of L^1 -norm and $W^{1,1}$ -norm. Therefore, we adopt the BiSecLG(1) refinement algorithm to promise the validity of Lemma 4.3. From numerical experiments, the performance of above adaptive algorithm with other refinement strategies liking red-green-blue refinement and newest vertex bisection is similar to that of the BiSecLG(1) refinement strategy.

Now we give the main result in this paper, namely the reliability and efficiency of η_l .

Theorem 4.1 Let Ω be an arbitrary polygonal domain. Assume (2.6) holds. If the mesh-size \overline{h}_l is small enough, the pointwise a posteriori error estimator η_l has the reliability and efficiency, up to some logarithmic factors, namely

$$||e_j||_{L^{\infty}(\Omega)} \lesssim \frac{|\ln \underline{h}_l|^2}{|\ln \overline{h}_l|} \frac{\lambda_{n+L}}{\lambda_{n+1}} \eta_l$$
 (4.3)

for any $j \in J$ and

$$\eta_l \lesssim \sqrt{L} \sum_{j \in J} ||e_j||_{L^{\infty}(\Omega)}.$$
(4.4)

The proof of (4.3) may be found in Corollary 4.7 in subsection 4.2, and (4.4) may be seen in Lemma 4.8 in subsection 4.3.

4.1 Proper approximation

Before the a posteriori error analysis, we shall briefly explain that $\Lambda_l u_j$ is a "proper" approximation of u_j $(j \in J)$ in some sense.

Lemma 4.2 Let $(\lambda_j, u_j) \in \mathbb{R}^+ \times W$ $(j \in J)$ be an eigenpair of (2.1), then we have

$$||u_i - \Lambda_l u_i||_{L^{\infty}(\Omega)} \lesssim ||u_i - R_l u_i||_{L^{\infty}(\Omega)}. \tag{4.5}$$

Proof. The triangle inequality directly leads to

$$||u_j - \Lambda_l u_j||_{L^{\infty}(\Omega)} \le ||u_j - R_l u_j||_{L^{\infty}(\Omega)} + ||R_l u_j - \Lambda_l u_j||_{L^{\infty}(\Omega)}.$$
(4.6)

Let $\tilde{x}_0 \in \tilde{T}_0$ satisfy $|(R_l u_j - \Lambda_l u_j)(\tilde{x}_0)| = ||R_l u_j - \Lambda_l u_j||_{L^{\infty}(\Omega)}$. Then there exists a regularized delta function $\tilde{\delta}_0$ satisfying

$$(\tilde{\delta}_0, v)_{\tilde{T}_0} = v(\tilde{x}_0) \ \forall \ v \in P_k(\tilde{T}_0), \ \|\tilde{\delta}_0\|_{W^{s,\infty}(\Omega)} \lesssim h_{\tilde{T}_0}^{-s-2}, s = 0, 1, 2, \dots$$

We may define a regularized Green's function \tilde{g}_0 as in (3.3). With the help of Lemmas 2.1 and 2.2, we have

$$||R_{l}u_{j} - \Lambda_{l}u_{j}||_{L^{\infty}(\Omega)} = |(R_{l}u_{j} - \Lambda_{l}u_{j}, \tilde{\delta}_{0})| = |a(R_{l}u_{j} - \Lambda_{l}u_{j}, R_{l}\tilde{g}_{0})|$$

$$= |a(u_{j} - \Lambda_{l}u_{j}, R_{l}\tilde{g}_{0})| = \lambda_{j}|(u_{j} - P_{l}u_{j}, R_{l}\tilde{g}_{0})|$$

$$\leq \lambda_{j}||u_{j} - P_{l}u_{j}||_{L^{2}(\Omega)}||R_{l}\tilde{g}_{0}||_{L^{2}(\Omega)}$$

$$\lesssim ||u_{j} - \Lambda_{l}u_{j}||_{L^{2}(\Omega)}||R_{l}\tilde{g}_{0}||_{L^{2}(\Omega)}$$

$$\lesssim ||u_{j} - R_{l}u_{j}||_{L^{2}(\Omega)}||R_{l}\tilde{g}_{0}||_{L^{2}(\Omega)}.$$

$$(4.7)$$

With a standard dual argument and using (3.8), we may deduce

$$||R_{l}\tilde{g}_{0}||_{L^{2}(\Omega)} \leq ||\tilde{g}_{0} - R_{l}\tilde{g}_{0}||_{L^{2}(\Omega)} + ||\tilde{g}_{0}||_{L^{2}(\Omega)}$$

$$\lesssim \overline{h}_{l}^{r} ||\tilde{g}_{0} - R_{l}\tilde{g}_{0}||_{H^{1}(\Omega)} + ||\tilde{g}_{0}||_{W^{1,p}(\Omega)}$$

$$\lesssim \overline{h}_{l}^{r} ||\tilde{g}_{0}||_{H^{1}(\Omega)} + ||\tilde{g}_{0}||_{W^{1,p}(\Omega)}$$

$$\lesssim 1 + \overline{h}_{l}^{r} \lesssim 1,$$

$$(4.8)$$

where $1 and <math>r < r_0$. Combining (4.6), (4.7) and (4.8), we may complete the proof of (4.5).

Remark 4.2 (An a priori L^{∞} -estimate) According to Lemma 4.2, we may obtain the a priori L^{∞} -estimate for elliptic eigenvalue problems. In particular, if Ω is convex, and the mesh is quusi-uniform, we have (see [35] and references therein)

$$||u_j - \Lambda_l u_j||_{L^{\infty}(\Omega)} \lesssim c_l \overline{h}_l \inf_{v_l \in V_l} ||u_j - v_l||_{W^{1,\infty}(\Omega)},$$

where $c_l = 1 + |\ln \overline{h}_l|$ for the linear element and $c_l = 1$ for higher-order elements. If Ω is non-convex and the mesh is local refined as in [28], we may obtain

$$||u_j - \Lambda_l u_j||_{L^{\infty}(\Omega)} \lesssim c_l \inf_{v_l \in V_l} ||u_j - v_l||_{L^{\infty}(\Omega)}.$$

Remark 4.3 We shall emphasize that the Ritz projection R_l generally loses the stability in the sense of L^{∞} -norm in non-convex domain, although $R_l u_j$ is the best approximation of u_j in the sense of the energy norm. It is difficult to find a (qausi-) optimal and computable approximation in the sense of L^{∞} -norm in highly graded meshes. Thus, with assuming that $R_l u_j$ is a "good" approximation of u_j , we deem that it is reasonable to regard $\Lambda_l u_j$ as a proper approximation of u_j in view of (4.5).

4.2 Reliability

We first review the weighted Sobolev stability of the L^2 -projection Q_l in [15], which provides a new method different from [6] to prove the reliability of η_l when $k \geq 2$. Let the mesh-size function h_l have the grading γ_l (see Definition 4.1 in [15]). We have the following weighted Sobolev stability of the L^2 -projection Q_l .

Lemma 4.3 Assume that

$$\gamma_l^{2+|1-\frac{2}{p}|} < \gamma_{max} := \frac{\sqrt{2k+2} + \sqrt{k}}{\sqrt{2k+2} - \sqrt{k}}.$$
(4.9)

Then the L^2 -projection Q_l has the weighted Sobolev stability

$$||h_l^{-2}Q_lv||_{L^p(\Omega)} \lesssim ||h_l^{-2}v||_{L^p(\Omega)} \quad \forall \ v \in L^p(\Omega)$$
 (4.10)

and

$$||h_l^{-1}\nabla Q_l v||_{L^p(\Omega)} \lesssim ||h_l^{-1}\nabla v||_{L^p(\Omega)} \quad \forall \ v \in W_0^{1,p}(\Omega)$$
 (4.11)

for $1 \leq p \leq \infty$.

For
$$j \in J$$
, let $x_0 \in \overline{\Omega}$ satisfy

$$|e_j(x_0)| = ||e_j||_{L^{\infty}(\Omega)}. (4.12)$$

For the subsequent analysis, our first step is to prove

$$||e_j||_{L^{\infty}(\Omega)} \lesssim |(\delta_0, e_j)|, \tag{4.13}$$

where δ_0 is defined in (3.1) and (3.2). We may use a similar argument as in [31] to get the following lemma. For simplicity, we omit the detailed proof.

Lemma 4.4 Let $0 < \alpha \le 1$ be the Hölder continuity exponent of the eigenfunction u_j . If the mesh-size \overline{h}_l is small enough, the following estimate holds

$$||e_j||_{L^{\infty}(\Omega)} \lesssim |(\delta_0, e_j)| + h_{T_0}^{\alpha\beta}, \tag{4.14}$$

where T_0 is an element containing x_0 and $\beta \geq 1$.

In order to drop the second term in (4.14), we use the a priori lower bound of $||e_j||_{L^{\infty}(\Omega)}$. Thanks to Lemmas 2.3 and 4.4, choosing $\beta > \frac{2}{\alpha} \frac{|\ln \underline{h}_l|}{|\ln \overline{h}_l|}$, we may deduce (4.13). Note that

$$||g_0||_{W^{2,1}(\Omega)} \lesssim \frac{|\ln \underline{h}_l|^2}{|\ln \overline{h}_l|}$$
 (4.15)

under the choice of β and in view of (3.4).

Next we shall derive the upper bound of $||e_i||_{L^{\infty}(\Omega)}$. Elementary algebraic manipulations lead to

$$(\delta_0, e_j) = a(e_j, g_0) = a(u_j, g_0) - a(\Lambda_l u_j, Q_l g_0) + a(\Lambda_l u_j, Q_l g_0 - g_0). \tag{4.16}$$

With the aid of Lemmas 2.1, 2.2 and 4.3, using the standard interpolation theory, we may obtain

$$a(e_{j}, g_{0}) = \lambda_{j} ((u_{j}, g_{0}) - (P_{l}u_{j}, Q_{l}g_{0})) + a(\Lambda_{l}u_{j}, Q_{l}g_{0} - g_{0})$$

$$= \lambda_{j} (u_{j} - P_{l}u_{j}, g_{0}) + a(\Lambda_{l}u_{j}, Q_{l}g_{0} - g_{0})$$

$$\lesssim \lambda_{j} \|u_{j} - P_{l}u_{j}\|_{L^{2}(\Omega)} \|g_{0}\|_{L^{2}(\Omega)}$$

$$+ \eta_{l,j}^{*} (\|h_{l}^{-2}(g_{0} - Q_{l}g_{0})\|_{L^{1}(\Omega)} + \|h_{l}^{-1}(g_{0} - Q_{l}g_{0})\|_{W^{1,1}(\Omega)})$$

$$\lesssim \|u_{j} - R_{l}u_{j}\|_{L^{2}(\Omega)} \|g_{0}\|_{L^{2}(\Omega)} + |g_{0}|_{W^{2,1}(\Omega)} \eta_{l,j}^{*}$$

$$\lesssim \|u_{j} - R_{l}u_{j}\|_{L^{2}(\Omega)} + \frac{|\ln \underline{h}_{l}|^{2}}{|\ln \overline{h}_{l}|} \eta_{l,j}^{*}.$$

$$(4.17)$$

In some a posteriori error analysis in the sense of energy norm (see [19]), $||u_j - R_l u_j||_{L^2(\Omega)}$ may be controlled by the a priori estimate

$$||u_j - R_l u_j||_{L^2(\Omega)} \lesssim \overline{h}_l^r ||u_j - R_l u_j||_{H^1(\Omega)},$$

where r > 0 is some regularity parameter. However, in the error analysis in the sense of L^{∞} -norm, it seems difficult to bound the L^2 -norm error through some a priori estimates. Instead, we may use some a posteriori estimates to bound this term.

Using the similar argument as in [31] and combining the weighted Sobolev stability of L^2 -projection, we may get the following a posteriori error estimate.

Lemma 4.5 Let u solve the source problem

$$\begin{cases}
-\Delta u = f & \text{in } \Omega, \\
u = 0 & \text{on } \partial\Omega.
\end{cases}$$
(4.18)

Then we have

$$||u - R_l u||_{L^p(\Omega)} \leq \hat{\eta}_{l,p}$$

for $4 , where <math>\hat{\eta}_{l,p}$ is defined as

$$\hat{\eta}_{l,p} := \inf_{v_l \in V_l} \left(\sum_{T \in \mathcal{T}_l} \left(\|h_T^2(f + \Delta R_l u + v_l)\|_{L^p(T)}^p + \|h_T^{1 + \frac{1}{p}} [\![\frac{\partial R_l u}{\partial n}]\!]\|_{L^p(\partial T \setminus \partial \Omega)}^p \right) \right)^{\frac{1}{p}}.$$

Proof. For $4 , let <math>\omega$ solve

$$\begin{cases} -\Delta\omega = \operatorname{sgn}(u - R_l u)|u - R_l u|^{p-1} & \text{in } \Omega, \\ \omega = 0 & \text{on } \partial\Omega. \end{cases}$$

By a standard dual argument, integrating by parts and using the interpolation theory, the trace theorem and (2.10), we deduce

$$\|u - R_l u\|_{L^p(\Omega)}^p = (u - R_l u, \operatorname{sgn}(u - R_l u)|u - R_l u|^{p-1})$$

$$= a(u - R_l u, \omega - Q_l \omega)$$

$$= \sum_{T \in \mathcal{T}_l} \left((u - R_l u, \omega - Q_l \omega)_T + \langle \llbracket \frac{\partial R_l u}{\partial n} \rrbracket, \omega - Q_l \omega \rangle_{\partial T \setminus \partial \Omega} \right)$$

$$\lesssim |\omega|_{W^{2,q}(\Omega)} \hat{\eta}_{l,p} \lesssim \|u - R_l u\|_{L^p(\Omega)}^{p-1} \hat{\eta}_{l,p},$$

where $\frac{1}{p} + \frac{1}{q} = 1$. Thus, we have

$$||u - R_l u||_{L^p(\Omega)} \lesssim \hat{\eta}_{l,p}$$

for any 4 .

Taking $u = u_j$, $f = \lambda_j u_j$ and $v_l = -\lambda_j R_l u_j + w_l$ for any $w_l \in V_l$, a direct triangle inequality leads to

$$||u_{j} - R_{l}u_{j}||_{L^{p}(\Omega)}^{p} \lesssim \inf_{w_{l} \in V_{l}} \sum_{T \in \mathcal{T}_{l}} \left(||h_{T}^{2}(\Delta R_{l}u_{j} + w_{l})||_{L^{p}(T)}^{p} + ||h_{T}^{1 + \frac{1}{p}}[\frac{\partial R_{l}u_{j}}{\partial n}]||_{L^{p}(\partial T \setminus \partial \Omega)}^{p} \right) + ||h_{l}^{2}\lambda_{j}(u_{j} - R_{l}u_{j})||_{L^{p}(\Omega)}^{p}$$

for $4 . For small enough <math>\overline{h}_l$, we may infer that

$$||u_j - R_l u_j||_{L^p(\Omega)} \lesssim \hat{\eta}_{l,j},\tag{4.19}$$

where $\hat{\eta}_{l,j}$ is defined as

$$\hat{\eta}_{l,j} := \inf_{w_l \in V_l} \max_{T \in \mathcal{T}_l} \left(h_T^2 \|\Delta R_l u_j + w_l\|_{L^{\infty}(T)}^p + h_T \| \left[\frac{\partial R_l u_j}{\partial n} \right] \|_{L^{\infty}(\partial T \setminus \partial \Omega)} \right).$$

Notice that (4.19) is valid for all 1 . Combining (4.13), (4.16), (4.17) and (4.19), we may conclude

$$||e_{j}||_{L^{\infty}(\Omega)} \lesssim \max_{T \in \mathcal{T}_{l}} \left(h_{T}^{2} ||\Delta(R_{l}u_{j} - \Lambda_{l}u_{j})||_{L^{\infty}(T)} + h_{T} ||\mathbb{I} \frac{\partial}{\partial n} (R_{l}u_{j} - \Lambda_{l}u_{j}) \mathbb{I}||_{L^{\infty}(\partial T \setminus \partial \Omega)} \right)$$

$$+ \frac{|\ln \underline{h}_{l}|^{2}}{|\ln \overline{h}_{l}|} \eta_{l,j}^{*}.$$

$$(4.20)$$

Now we show that the first term in (4.20) is a higher order quantity.

Lemma 4.6 For any $T \in \mathcal{T}_l$, it holds that

$$\|\nabla (R_l u_j - \Lambda_l u_j)\|_{L^{\infty}(T)} \lesssim h_T^{-1} \overline{h}_l^r \|e_j\|_{L^{\infty}(\Omega)}$$

$$\tag{4.21}$$

and

$$\|\Delta(R_l u_i - \Lambda_l u_i)\|_{L^{\infty}(T)} \lesssim h_T^{-2} \overline{h}_l^r \|e_i\|_{L^{\infty}(\Omega)}$$

$$\tag{4.22}$$

for any $r < r_0$.

Proof. For any $T \in \mathcal{T}_l$, let $x_T \in T$ satisfy

$$\|\nabla (R_l u_j - \Lambda_l u_j)\|_{L^{\infty}(T)} \lesssim \sup_{\nu} |(\nabla (R_l u_j - \Lambda_l u_j) \cdot \nu)(x_T)|,$$

where ν is an arbitrary direction vector. Let δ_1 be defined as in (3.5) associated with x_T . Using Lemmas 2.2 and 3.3, we deduce

$$(\nabla (R_{l}u_{j} - \Lambda_{l}u_{j}) \cdot \nu)(x_{T}) = (R_{l}u_{j} - \Lambda_{l}u_{j}, \nabla \delta_{1} \cdot \nu)$$

$$= a(R_{l}u_{j} - \Lambda_{l}u_{j}, R_{l}g_{1}) = \lambda_{j}(u_{j} - P_{l}u_{j}, R_{l}g_{1})$$

$$\leq ||u_{j} - P_{l}u_{j}||_{L^{2}(\Omega)} ||R_{l}g_{1}||_{L^{2}(\Omega)}$$

$$\leq ||u_{j} - \Lambda_{l}u_{j}||_{L^{2}(\Omega)} ||R_{l}g_{1}||_{L^{2}(\Omega)}$$

$$\lesssim h_{T}^{-1}\overline{h}_{l}^{T} ||e_{j}||_{L^{\infty}(\Omega)}$$

for any $r < r_0$, which leads to (4.21). Then we may get (4.22) through a standard inverse estimate.

Corollary 4.7 (Reliability) Assume (2.6) holds. If the mesh-size \overline{h}_l is small enough, it holds that

$$||e_j||_{L^{\infty}(\Omega)} \lesssim \frac{|\ln \underline{h}_l|^2}{|\ln \overline{h}_l|} \frac{\lambda_{n+L}}{\lambda_{n+1}} \eta_l$$

for any $j \in J$.

Proof. Combining (4.20) and Lemma 4.6, we get

$$||e_j||_{L^{\infty}(\Omega)} \lesssim \frac{|\ln \underline{h}_l|^2}{|\ln \overline{h}_l|} \eta_{l,j}^*.$$

We expand $\Lambda_l u_j = \sum_{i \in J} \alpha_i u_{l,i}$ with coefficients $\alpha_i = (R_l u_k, u_{l,i}) = \lambda_{l,i}^{-1} \lambda_j(u_j, u_{l,i}) \leq \frac{\lambda_{n+L}}{\lambda_{n+1}}$. Taking $v_l = \sum_{i \in J} \alpha_i \lambda_{l,i} u_{l,i}$ in (4.2) and using the triangle inequality, we complete the proof.

Remark 4.4 Note that $\Delta \Lambda_l u_j = 0$ when the linear element is used. Taking $v_l = 0$ in η_l^* , with a similar argument, we may obtain that

$$\|e_j\|_{L^{\infty}(\Omega)} \lesssim \frac{|\ln \underline{h}_l|^2}{|\ln \overline{h}_l|} \frac{\lambda_{n+L}}{\lambda_{n+1}} \left(\max_{T \in \mathcal{T}_l} h_T \sum_{i \in J} \| [\![\frac{\partial u_{l,i}}{\partial n}]\!] \|_{L^{\infty}(\partial T \setminus \partial \Omega)} \right).$$

In other words, the jump flux residuals dominate the a posterori error when k = 1.

4.3 Efficiency

In this subsection, we give the proof of efficiency of η_l .

Lemma 4.8 (Efficiency) If the mesh-size \overline{h}_l is small enough, it holds that

$$\eta_l \lesssim \sqrt{L} \sum_{j \in J} ||e_j||_{L^{\infty}(\Omega)}.$$

Proof. We modify the local argument in [31, 38] and use some results in [6]. Let b_T be the usual bubble function, i.e., the polynomial of degree three, obtained by the product of the barycentric coordinates of T. Note that (see [38])

$$||b_T||_{W^{s,1}(T)} \lesssim h_T^{2-s}.$$

Integrating by parts, for any $v \in V$, we have

$$a(e_j, v) = (e_j, -\Delta v) + \sum_{T \in \mathcal{T}_i} \langle e_j, \frac{\partial v}{\partial n} \rangle_{\partial T}$$

and

$$a(e_j, v) = (\lambda_j u_j + \Delta \Lambda_l u_j, v) + \sum_{T \in \mathcal{T}_l} \langle v, \frac{\partial e_j}{\partial n} \rangle_{\partial T}.$$

Taking $v = (\lambda_j P_l u_j + \Delta \Lambda_l u_j) b_T$ and using the trace theorem, we get

$$h_{T}^{2} \|\lambda_{j} P_{l} u_{j} + \Delta \Lambda_{l} u_{j} \|_{L^{\infty}(T)} \lesssim h_{T} \|u_{j} - P_{l} u_{j} \|_{L^{2}(T)} + \|e_{j}\|_{L^{\infty}(T)}$$

$$\lesssim h_{T} \|u_{j} - \Lambda_{l} u_{j} \|_{L^{2}(\Omega)} + \|e_{j} \|_{L^{\infty}(T)}$$

$$\lesssim \|e_{j} \|_{L^{\infty}(\Omega)}.$$
(4.23)

Given an interior edge E, we denote by T_1 and T_2 the two elements that share the edge E. Let φ_E be a piecewise quadratic polynomial on $T_1 \cup T_2$, which is one at the midpoint of E and vanishes on the other edges of $T_1 \cup T_2$. Taking $v = \begin{bmatrix} \frac{\partial \Lambda_l u_j}{\partial n} \end{bmatrix} \varphi_E$, with a similar argument as in proving (4.23), we obtain

$$h_E \| \left[\frac{\partial \Lambda_l u_j}{\partial n} \right] \|_{L^{\infty}(E)} \lesssim \|e_j\|_{L^{\infty}(\Omega)}. \tag{4.24}$$

Owing to Lemma 1 in [6], we have

$$\sum_{j \in J} \lVert \lambda_{l,j} u_{l,j} + \Delta u_{l,j} \rVert_{L^2(T)}^2 \lesssim \sum_{j \in J} \lVert \lambda_j P_l u_j + \Delta \Lambda_l u_j \rVert_{L^2(T)}^2$$

for any $T \in \mathcal{T}_l$, and

$$\sum_{i \in I} \| \left\| \frac{\partial u_{l,j}}{\partial n} \right\| \|_{L^2(E)}^2 \lesssim \sum_{i \in I} \| \left\| \frac{\partial \Lambda_l u_j}{\partial n} \right\| \|_{L^2(E)}^2$$

for any interior edge E. Using the Hölder inequality and the stand inverse inequality, and combining (4.23) and (4.24), we deduce

$$\eta_l^2(T) \lesssim L \sum_{j \in J} \|e_j\|_{L^\infty(\Omega)}^2 \lesssim L(\sum_{j \in J} \|e_j\|_{L^\infty(\Omega)})^2,$$

which gives the efficiency of η_l in view of $\eta_l = \max_{T \in \mathcal{T}_l} \eta_l(T)$.

5 Numerical experiments

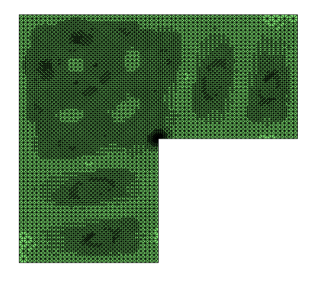
In this section, we present some benchmarks of numerical experiments in non-convex domains where some eigenfunctions have singularities. Specifically, we approximate (2.1) in different domains with the linear conforming element by the adaptive algorithm proposed in section 4.1. We set the bulk parameter $\theta = 0.5$ in all adaptive computations.

5.1 Approximation on L-shaped domain

We start our numerical experiments with the approximation in L-shaped domain

$$\Omega_1 = (0,1)^2 \setminus ([\frac{1}{2},1) \times (0,\frac{1}{2}]).$$

The initial mesh \mathcal{T}_0 is an uniform mesh with $h_T = |T|^{\frac{1}{2}} = \frac{\sqrt{2}}{16}$ for all elements. By the adaptive algorithm, it may be seen that λ_{12} is close to λ_{13} and the eigenfunction u_{12} (associated with λ_{12}) has local singularities. Thus, in this experiment, we take $J = \{12, 13\}$. Figure 1 shows the adaptive mesh with 19700 elements, from which we can see that our adaptive algorithm captures the singularities especially around the reentrant corner accurately. Figure 2 shows that the convergence rate of η_l is $O(N^{-1})$, which is quasi-optimal. Moreover, from Table 1 we may see that the product of N_l and η_l is gradually stable around a certain constant, which illustrates that η_l is $O(N^{-1})$.



10²
10³
10⁴
10²
10³
10⁴
10⁵
10⁶

Fig. 1. The adaptive mesh with 19700 elements in Ω_1 for the 12th and 13th eigenpairs.

Fig. 2. The blue dots represent the pointwise a posteriori error estimator η_l for $J = \{12, 13\}$ in Ω_1 . The dotted line represents the fitted convergence rate.

mesh level	degrees of freedom	a posteriori error	product
l	N_l	η_l	$N_l imes \eta_l$
0	33	37.768	1246.3
4	469	2.2696	1064.4
8	2625	0.47195	1251.6
12	7508	0.17591	1320.7
16	18981	0.068936	1308.5

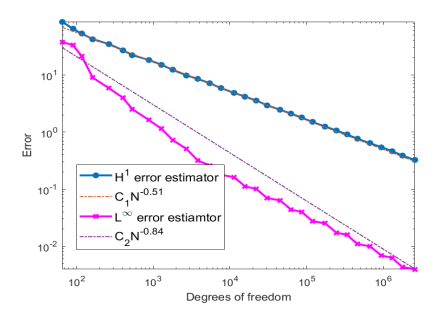
Table 1: Degrees of freedom, the a posteriori error and their product in L-shape domain Ω_1 for 12th and 13th eigenpairs on different mesh levels.

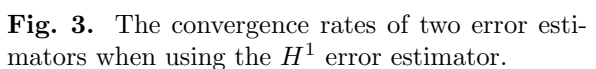
Next, we present some numerical results to illustrate that when we limit the a prior error in the sense of L^{∞} -norm in practical applications, it is better to use the L^{∞} error estimator. To show this, we introduce the H^1 error estimator defined in [19]

$$\eta_{l}^{a}(T) = \left(\sum_{j \in J} h_{T}^{2} \|\lambda_{l,j} u_{l,j}\|_{L^{2}(T)}^{2} + \sum_{j \in J} h_{T} \| \left[\frac{\partial u_{l,j}}{\partial n} \right] \|_{L^{2}(\partial T \setminus \partial \Omega)}^{2} \right)^{\frac{1}{2}}$$

and

$$\eta_l^a = (\sum_{T \in \mathcal{T}_l} \eta_l^a(T)^2)^{\frac{1}{2}}.$$





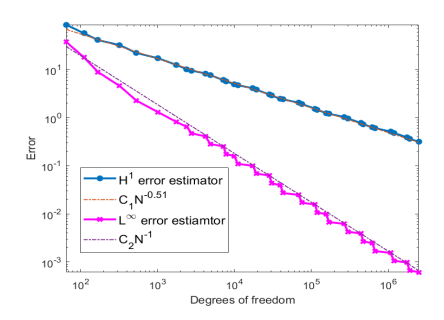


Fig. 4. The convergence rates of two error estimators when using the L^{∞} error estimator.

When we use the H^1 error estimator, we rely on Dörfler marking in Mark. First we use the H^1 error estimator in the adaptive algorithm. In each iteration, we also record the value of the L^{∞} error estimator (it may be seen as the a priori L^{∞} error in view of the reliability and efficiency of the L^{∞} error estimator). Figure 3 shows that when the H^1 error estimator is used, the convergence rate of the L^{∞} error estimator becomes suboptimal. In other words, we need more degrees of freedom to limit the a priori error in the sense of L^{∞} -norm. Then, we use the L^{∞} error estimator as the a posteriori error estimator in the adaptive algorithm. We also record the value of the H^1 error estimator in each iteration (it may be seen as the a priori H^1 error). Figure 4 shows that the convergence rate of the H^1 error estimator keeps optimal. This experiment illustrates that we may get the optimal convergence rate of the a priori error in the sense of energy norm by using the L^{∞} error estimator.

5.2 Approximation on a symmetric slit domain

In this subsection, numerical experiments are set in a square domain with four symmetric slits defined as

$$\begin{split} \Omega_2 = & (-1,1)^2 \backslash (\operatorname{conv}\{(0.5,0),(1,0)\} \cup \operatorname{conv}\{(0,0.5),(0,1)\} \\ & \cup \operatorname{conv}\{(-0.5,0),(-1,0)\} \cup \operatorname{conv}\{(0,-0.5),(0,-1)\}), \end{split}$$

where $\operatorname{conv}\{(a_1,b_1),(a_2,b_2)\}$ denotes the line segment with (a_1,b_1) and (a_2,b_2) as the endpoints.

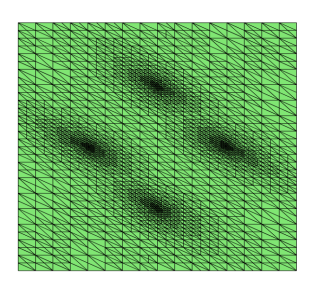


Fig. 5. The adaptive mesh with 5373 elements in Ω_2 for the 2nd and 3rd eigenpairs.

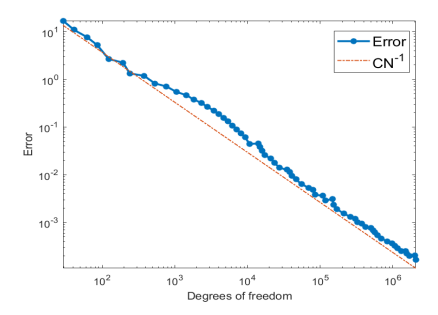


Fig. 6. The blue dots represent the pointwise a posteriori error estimator η_l for $J = \{2,3\}$ in Ω_2 . The dotted lines represent the fitted convergence rate.

It is known that the interior eigenvalues $\lambda_2 = \lambda_3$ (see [19]). We restrict our attention on computations for the second and third eigenpairs, i.e., $J = \{2, 3\}$. Figure 5 shows the adaptive mesh with 5373 elements, which illustrates that our adaptive algorithm captures the singularities around four slits accurately. Figure

6 shows that the convergence rate of the pointwise a posteriori error estimator η_l is quasi-optimal. This experiment illustrates the pointwise a posteriori error estimator η_l is still reliable and efficiency for multiple eigenvalues.

5.3 Approximation on a perturbed slit domain

In this subsection, we study a perturbation of the geometry and show that the refinement strategy may exert a significant impact on the performance of the performance of the entire adaptive algorithm. Specifically, we consider the slit domain

$$\Omega_3 = (-1, 1)^2 \setminus (\operatorname{conv}\{(0.505, 0), (1, 0)\} \cup \operatorname{conv}\{(0, 0.501), (0, 1)\} \cup \operatorname{conv}\{(-0.499, 0), (-1, 0)\} \cup \operatorname{conv}\{(0, -0.5), (0, -1)\}).$$

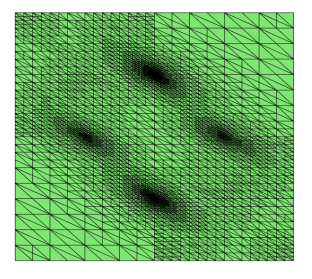


Fig. 7. The adaptive mesh with 5852 elements in Ω_3 for the 2nd eigenpair by using the BiSecLG(1) refinement strategy.

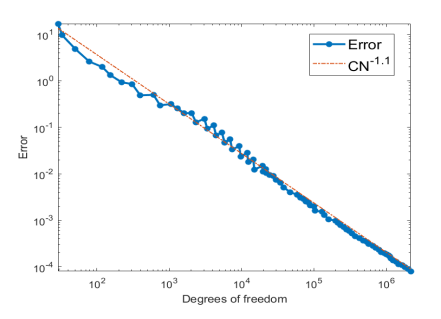


Fig. 8. The blue dots represent the pointwise a posteriori error estimator η_l for $J = \{2\}$ in Ω_3 . The dotted lines represent the fitted convergence rate.

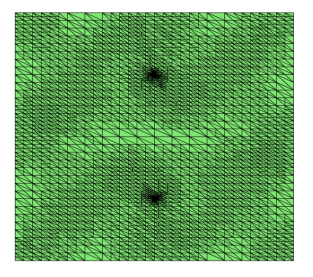


Fig. 9. The adaptive mesh with 5858 elements in Ω_3 for the 2nd eigenpair by using the newest vertex refinement strategy.

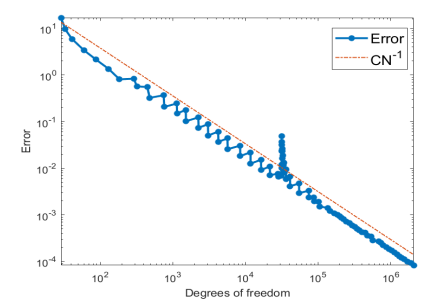


Fig. 10. The blue dots represent the pointwise a posteriori error estimator η_l for $J = \{2\}$ in Ω_3 . The dotted lines represent the fitted convergence rate.

We observed an interesting phenomenon when applying the adaptive finite element method to solve clustered eigenvalue problems with different refinement strategies in Figures 7 and 9. When we only choose $J = \{2\}$ and use the adaptive algorithm in section 4, we may see that the singularities around four slits are all captured, and the convergence of η_l is optimal (as shown in Figures 7 and 8). However, if we use the newest vertex refinement strategy, only two singularities are captured, and the convergence history of η_l seems problematic when degrees of freedom within the range of 10^4 to 10^5 (as shown in Figures 9 and 10). When we choose $J = \{2,3\}$, i.e., a whole cluster of eigenvalues, this problem is

cured. No matter whether we use the newest vertex refinement or BiSecLG(1) refinement, the adaptive algorithm captures the singularities around four slits (Figures 11 and 13), and the convergence rate of η_l keeps optimal as shown in Figures 12 and 14. This comparative experiment explains why our adaptive algorithm is more robust in the sense that it only requires some gap conditions of the cluster from the remaining spectrum, but no gap within the cluster. And this experiment demonstrates that we should choose a whole cluster to construct the a posteriori error estimator in practical applications.

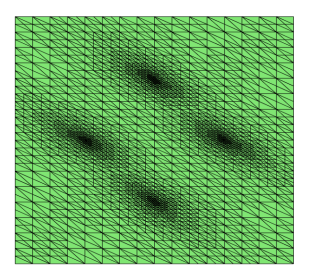


Fig. 11. The adaptive mesh with 5304 elements in Ω_3 for the 2nd and 3rd eigenpairs by using the BiSecLG(1) refinement strategy.

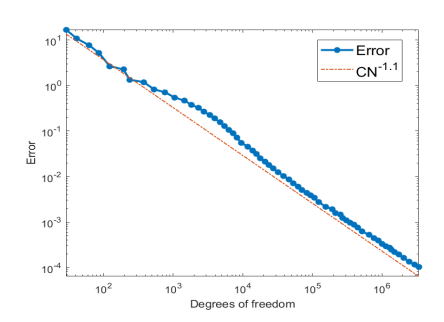


Fig. 12. The blue dots represent the pointwise a posteriori error estimator η_l for $J = \{2,3\}$ in Ω_3 . The dotted lines represent the fitted convergence rate.

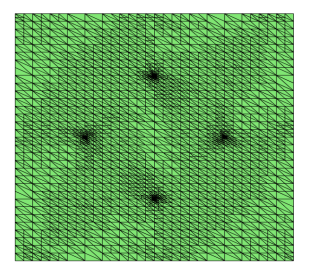


Fig. 13. The adaptive mesh with 4251 elements in Ω_3 for the 2nd and 3rd eigenpairs by using the newest vertex refinement strategy.

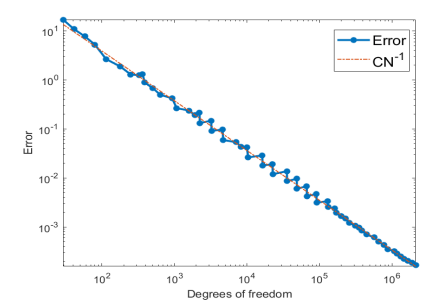


Fig. 14. The blue dots represent the pointwise a posteriori error estimator η_l for $J = \{2,3\}$ in Ω_3 . The dotted lines represent the fitted convergence rate.

6 Conclusion

In this paper, we propose and analyze a pointwise a posteriori error estimator for conforming finite element approximations of eigenvalue clusters of second-order elliptic eigenvalue problems with AFEMs. It is proven that the pointwise a posteriori error estimator is reliable and efficient, which is also extended to higher order elements with the help of the weighted Sobolev stability of the L^2 - projection. Specially, jump residuals dominate the total a posteriori error when the linear element is used. Numerical results verify our theoretical findings.

References

[1] R. A. Adams. *Sobolev spaces*. Pure and Applied Mathematics. Academic Press [Harcourt Brace Jovanovich, Publishers], New York-London, 1975.

- [2] M. Ainsworth and J. T. Oden. A posteriori error estimation in finite element analysis. *Comput. Methods Appl. Mech. Engrg.*, 142(1-2):1–88, 1997.
- [3] I. Babuška and W. C. Rheinboldt. Error estimates for adaptive finite element computations. SIAM J. Numer. Anal., 15(4):736–754, 1978.
- [4] I. Babuška and M. Vogelius. Feedback and adaptive finite element solution of one-dimensional boundary value problems. *Numer. Math.*, 44(1):75–102, 1984.
- [5] N. Y. Bakaev, V. Thomée, and L. B. Wahlbin. Maximum-norm estimates for resolvents of elliptic finite element operators. *Math. Comp.*, 72(244):1597–1610, 2003.
- [6] A. Bonito and A. Demlow. Convergence and optimality of higher-order adaptive finite element methods for eigenvalue clusters. SIAM J. Numer. Anal., 54(4):2379–2388, 2016.
- [7] E. Cancès, G. Dusson, Y. Maday, B. Stamm, and M. Vohralík. Guaranteed a posteriori bounds for eigenvalues and eigenvectors: multiplicities and clusters. *Math. Comp.*, 89(326):2563–2611, 2020.
- [8] C. Carstensen. A unifying theory of a posteriori finite element error control. Numer. Math., 100(4):617–637, 2005.
- [9] Z. Chen and R. H. Nochetto. Residual type a posteriori error estimates for elliptic obstacle problems. *Numer. Math.*, 84(4):527–548, 2000.
- [10] X. Dai, L. He, and A. Zhou. Convergence and quasi-optimal complexity of adaptive finite element computations for multiple eigenvalues. IMA J. Numer. Anal., 35(4):1934–1977, 2015.
- [11] X. Dai, J. Xu, and A. Zhou. Convergence and optimal complexity of adaptive finite element eigenvalue computations. *Numer. Math.*, 110(3):313–355, 2008.
- [12] E. Dari, R. G. Durán, and C. Padra. Maximum norm error estimators for three-dimensional elliptic problems. SIAM J. Numer. Anal., 37(2):683–700, 2000.
- [13] M. Dauge. Elliptic Boundary Value Problems on Corner Domains. Lecture Notes in Mathematics. Springer-Verlag, Berlin, 1988.
- [14] A. Demlow, J. Guzmán, and A. H. Schatz. Local energy estimates for the finite element method on sharply varying grids. *Math. Comp.*, 80(273):1–9, 2011.
- [15] L. Diening, J. Storn, and T. Tscherpel. On the Sobolev and L^p -stability of the L^2 -projection. SIAM J. Numer. Anal., 59(5):2571–2607, 2021.
- [16] L. C. Evans. Partial differential equations. Graduate Studies in Mathematics. American Mathematical Society, Providence, RI, second edition, 2010.
- [17] D. A. French, S. Larsson, and R. H. Nochetto. Pointwise a posteriori error analysis for an adaptive penalty finite element method for the obstacle problem. *Comput. Methods Appl. Math.*, 1(1):18–38, 2001.
- [18] D. Gallistl. Adaptive nonconforming finite element approximation of eigenvalue clusters. *Comput. Methods Appl. Math.*, 14(4):509–535, 2014.
- [19] D. Gallistl. An optimal adaptive FEM for eigenvalue clusters. Numer. Math., 130(3):467–496, 2015.
- [20] S. Giani and I. G. Graham. A convergent adaptive method for elliptic eigenvalue problems. SIAM J. Numer. Anal., 47(2):1067–1091, 2009.
- [21] P. Grisvard. *Elliptic Problems in Nonsmooth Domains*. Monographs and Studies in Mathematics. Pitman (Advanced Publishing Program), Boston, MA, 1985.
- [22] L. Grubišić and J. S. Ovall. On estimators for eigenvalue/eigenvector approximations. *Math. Comp.*, 78(266):739–770, 2009.
- [23] V. Heuveline and R. Rannacher. A posteriori error control for finite approximations of elliptic eigenvalue problems. *Adv. Comput. Math.*, 15(1-4):107–138 (2002), 2001.
- [24] R. H. W. Hoppe, H. Wu, and Z. Zhang. Adaptive finite element methods for the Laplace eigenvalue problem. J. Numer. Math., 18(4):281–302, 2010.

- [25] T. Kashiwabara and T. Kemmochi. Pointwise error estimates of linear finite element method for Neumann boundary value problems in a smooth domain. *Numer. Math.*, 144(3):553–584, 2020.
- [26] M. G. Larson. A posteriori and a priori error analysis for finite element approximations of self-adjoint elliptic eigenvalue problems. SIAM J. Numer. Anal., 38(2):608–625, 2000.
- [27] D. Leykekhman and B. Vexler. A priori error estimates for three dimensional parabolic optimal control problems with pointwise control. SIAM J. Control Optim., 54(5):2403–2435, 2016.
- [28] B. Li. Maximum-norm stability of the finite element method for the Neumann problem in nonconvex polygons with locally refined mesh. *Math. Comp.*, 91(336):1533–1585, 2022.
- [29] Z. Li, Q. Liang, and X. Xu. Pointwise a posteriori error estimators for elliptic eigenvalue problems. arXiv.2511.06815, 2025.
- [30] J. A. Nitsche. L_{∞} -convergence of finite element approximation. In *Journées "Éléments Finis"* (Rennes, 1975), page 18. Univ. Rennes, Rennes, 1975.
- [31] R. H. Nochetto. Pointwise a posteriori error estimates for elliptic problems on highly graded meshes. *Math. Comp.*, 64(209):1–22, 1995.
- [32] R. H. Nochetto, M. Paolini, and C. Verdi. An adaptive finite element method for two-phase Stefan problems in two space dimensions. I. Stability and error estimates. *Math. Comp.*, 57(195):73–108, S1–S11, 1991.
- [33] A. H. Schatz, I. H. Sloan, and L. B. Wahlbin. Superconvergence in finite element methods and meshes that are locally symmetric with respect to a point. SIAM J. Numer. Anal., 33(2):505–521, 1996.
- [34] A. H. Schatz and L. B. Wahlbin. On the quasi-optimality in L_{∞} of the \dot{H}^1 -projection into finite element spaces. *Math. Comp.*, 38(157):1–22, 1982.
- [35] L. R. Scott. Optimal L^{∞} estimates for the finite element method on irregular meshes. Math. Comp., 30(136):681-697, 1976.
- [36] S. M. Shen and T. Lü. Maximum norm estimates of approximate eigenfunctions by finite element methods and the correction accelerations. *Math. Numer. Sinica*, 8(1):12–17, 1986.
- [37] Z. Shen. Bounds of Riesz transforms on L^p spaces for second order elliptic operators. Ann. Inst. Fourier (Grenoble), 55(1):173-197, 2005.
- [38] R. Verfürth. A posteriori error estimators for the Stokes equations. Numer. Math., 55(3):309–325, 1989.